

Simple Establishment of a Vascularized Osteogenic Bone Marrow Niche Using Pre-Cast Poly(ethylene Glycol) (PEG) Hydrogels in an Imaging Microplate

Lisa A. Krattiger¹, Maria Mitsi², Benjamin R. Simona², Martin Ehrbar¹

¹Department of Obstetrics, University Hospital Zurich, University of Zurich ²Ectica Technologies AG

Corresponding Author

Martin Ehrbar

martin.ehrbar@usz.ch

Citation

Krattiger, L.A., Mitsi, M., Simona, B.R., Ehrbar, M. Simple Establishment of a Vascularized Osteogenic Bone Marrow Niche Using Pre-Cast Poly(ethylene Glycol) (PEG) Hydrogels in an Imaging Microplate. *J. Vis. Exp.* (195), e65413, doi:10.3791/65413 (2023).

Date Published

May 19, 2023

DOI

10.3791/65413

URL

jove.com/video/65413

Abstract

The bone and bone marrow are highly vascularized and structurally complex organs, and are sites for cancer and metastasis formation. *In vitro* models recapitulating bone- and bone marrow-specific functions, including vascularization, that are compatible with drug screening are highly desirable. Such models can bridge the gap between simplistic, structurally irrelevant two-dimensional (2D) *in vitro* models and the more expensive, ethically challenging *in vivo* models. This article describes a controllable three-dimensional (3D) co-culture assay based on engineered poly(ethylene glycol) (PEG) matrices for the generation of vascularized, osteogenic bone-marrow niches. The PEG matrix design allows the development of 3D cell cultures through a simple cell seeding step requiring no encapsulation, thus enabling the development of complex co-culture systems. Furthermore, the matrices are transparent and pre-cast onto glass-bottom 96-well imaging plates, rendering the system suitable for microscopy. For the assay described here, human bone marrow-derived mesenchymal stromal cells (hBM-MSCs) are cultured first until a sufficiently developed 3D cell network is formed. Subsequently, GFP-expressing human umbilical vein endothelial cells (HUVECs) are added. The culture development is followed by bright-field and fluorescence microscopy. The presence of the hBM-MSC network supports the formation of vascular-like structures that otherwise would not form and that remain stable for at least 7 days. The extent of vascular-like network formation can easily be quantified. This model can be tuned toward an osteogenic bone-marrow niche by supplementing the culture medium with bone morphogenetic protein 2 (BMP-2), which promotes the osteogenic differentiation of the hBM-MSCs, as assessed by increased alkaline phosphatase (ALP) activity at day 4 and day 7 of co-culture. This cellular model can be used as a platform for culturing various cancer cells and studying how they interact with bone- and bone marrow-specific vascular

niches. Moreover, it is suitable for automation and high-content analyses, meaning it would enable cancer drug screening under highly reproducible culture conditions.

Introduction

The bone and bone marrow are structurally and functionally complex organs central to human health. This is reflected by the existence of distinct niches that regulate hematopoiesis and bone maintenance¹. It is now widely accepted that in healthy bone marrow, the maintenance and expansion of hematopoietic and skeletal stem cells, as well as their progeny, are controlled by distinct niches. These niches comprise various cell types, including osteolineage cells, mesenchymal stem cells, endothelial and perivascular cells, neuronal and glial cells, adipocytes, osteoclasts, macrophages, and neutrophils². Not surprisingly, these mostly vasculature-associated niches are also involved in the development of various types of leukemia³ and are the site of metastasis for different cancers⁴. Owing to its specific roles in bone formation, remodeling, and bone (marrow) maintenance, the bone-associated vasculature has distinct specialized structures different from the vasculature found elsewhere in the body^{5,6,7}. Thus, anti-angiogenic or vasculature-modulating drugs applied systemically may have different effects within these specialized environments⁸. Therefore, models to investigate the molecular mechanisms involved in maintaining the bone and bone marrow physiological properties, bone and bone marrow regeneration, and responses to therapeutic treatments are highly desirable.

Classical two-dimensional (2D) tissue cultures and *in vivo* investigations using animal models have provided invaluable insight into the roles of different cells and molecular players involved in the development of bone and bone marrow^{9,10}.

Models that allow for high-throughput experiments with relevant human cells could improve our understanding of how to modulate selected parameters in these highly complex systems.

In the past decade, principles derived from tissue engineering have been employed to generate 3D tissue models^{11,12}. These have mostly relied on the encapsulation of tissue-relevant cells into biomaterials to establish 3D mono- or co-cultures¹³. Among the most used biomaterials are fibrin¹⁴, collagen¹⁵, and Matrigel^{16,17}, all of which are highly biocompatible and provide appropriate conditions for the growth of many cell types. These biomaterials have the ability to generate *in vitro* models that recapitulate key aspects of the different vascular niches found *in vivo*¹⁸. Moreover, the use of microfluidic devices to generate perfused vascular bone and bone marrow models has contributed to the generation of *in vitro* models of higher complexity^{19,20,21,22}.

The difficulty in controlling the composition and engineering the properties of naturally occurring biomaterials has inspired the development of synthetic analogs that can be rationally designed with predictable physical, chemical, and biological properties^{23,24}. We have developed fully synthetic factor XIII (FXIII) cross-linked poly(ethylene glycol) (PEG)-based hydrogels, which are functionalized with RGD peptides and matrix metalloprotease (MMP) cleavage sites to facilitate cell attachment and remodeling^{25,26}. The modular design of these biomaterials has been successfully used to optimize

conditions for the formation of 3D vascularized bone and bone marrow models^{27,28}.

For the testing of larger numbers of different culture conditions and new therapeutics, models with a higher throughput capability are required. We have recently shown that the FXIII cross-linking of our PEG hydrogel can be controlled through an electrochemical process such that an in-depth hydrogel stiffness gradient is formed²⁹. When cells are added on top of such hydrogels, they migrate toward the interior and gradually develop into highly interconnected 3D cellular networks³⁰. The elimination of the need to encapsulate cells into the hydrogel, which is usually present with other 3D scaffolds, not only simplifies the experimental design but also allows the sequential addition of different cell types at different time points to generate complex co-culture systems. These hydrogels are available pre-cast onto glass-bottom 96-well imaging plates, thus making the establishment of 3D cultures achievable by manual as well as automated cell seeding protocols. The optical transparency of the PEG hydrogels renders the platform compatible with microscopy.

Here, we present a straightforward method for the generation and characterization of vascularized osteogenic niches within this ready-to-use, synthetic plug-and-play platform. We show that the development of vascular networks can be stimulated with a growth factor commonly used for inducing *in vitro* osteogenesis, bone morphogenetic protein-2 (BMP-2), while osteogenic differentiation can be prevented by supplementation of fibroblast growth factor 2 (FGF-2)^{27,31}. The networks formed are different when compared to FGF-2-stimulated networks in terms of the overall appearance, as well as the cell and ECM distribution. Moreover, we monitored the osteogenic induction using alkaline phosphatase as a marker. We demonstrate the increased expression of this

marker over time and compare the expression to that in FGF-2 stimulated networks using qualitative and quantitative methods. Finally, we demonstrate the suitability of the generated niches of this model for two potential applications. Firstly, we performed a proof-of-concept drug sensitivity assay by adding bevacizumab to pre-formed niches and monitoring the degradation of the vascular networks in its presence. Secondly, we added MDA-MB-231 breast cancer and U2OS osteosarcoma cells to pre-formed osteogenic niches, showing that the niches can be used to study interactions between cancer cells and their environment.

Protocol

Figure 1 summarizes the following protocol sections.

1. Establishing the 3D stromal monoculture

1. Prepare the hBM-MSC cell suspension.
 1. Grow hBM-MSCs to a confluence level of 70%-90% in MEM α supplemented with 10% FBS, 1% penicillin-streptomycin, and 5 ng/mL FGF-2 in an incubator at 37 °C and 5% CO₂ in a humidified atmosphere. The cells may be used up to passage 6.
 2. Wash the cells with PBS, and detach them using 0.05% Trypsin-EDTA for 3-5 min at 37 °C. Stop the detachment process by flushing with basal medium (MEM α supplemented with 10% FBS and 1% penicillin-streptomycin). Collect the suspended cells in a 50 mL conical centrifuge tube.
 3. Count the cells using a hemacytometer or an automated cell counter, and determine the total number of cells in the suspension.
 4. Pellet the cells by centrifugation at 200 x g for 5 min. Carefully remove the supernatant.

5. Resuspend the cells in an appropriate volume of basal medium to achieve a concentration of 1×10^7 cells/mL of stock solution.
 6. Prepare 50 mL conical centrifuge tubes containing the required volume of basal medium supplemented with the respective growth factors (FGF-2 and BMP-2 at defined concentrations, e.g., 0 ng/mL, 25 ng/mL, 50 ng/mL, 100 ng/mL, or 200 ng/mL). Per well, 200 μ L is required. If cell seeding is to be performed using an automated liquid handler, also consider the dead volume of the instrument. For manual cell seeding, a volume excess of 10% is sufficient.
 7. Add the hBM-MSCs from the stock solution at a dilution of 1:66.67 to achieve a concentration of 1.5×10^5 cells/mL.
2. Prepare the plate for seeding.
 1. Remove the polypropylene adhesive film covering the 96-well hydrogel plate.
 2. Carefully aspirate the storage buffer covering the hydrogels. For this task, use a microplate washer; however, manual handling is possible.
 1. When using a manual aspirator or multichannel pipette, position the tip against the wall of the well, and slowly move down toward the edge of the inner well while aspirating the buffer. This will avoid damaging the hydrogel surface.
 2. When using an automated plate washer, set the aspiration nozzles at least 3.8 mm from the plate carrier (this corresponds to 0.8 mm from the inner ring of the hydrogel plate) and toward the edge of the well. Refer to

the manufacturer's manual for more detailed instructions and to obtain the plate drawings of the 96-well hydrogel plate.

3. Add 200 μ L/well of the cell suspension prepared in step 1.1.7 after thoroughly mixing to ensure the cells are homogeneously distributed. During seeding, to avoid uneven sedimentation of the cells in one region of the substrate, do not tilt the plate. For manual seeding, periodically mix the cell suspension (after seeding three wells) to keep the mixture homogeneous. For automated seeding, mix with a serological pipet immediately before dispensing in order to dispense volumes containing equal numbers of cells.
4. Maintain the cultures at 37 °C and 5% CO₂ in a humidified atmosphere.
5. Monitor the development of the cultures by bright-field microscopy with a 5x objective as desired. Acquire reference images approximately 30 min after seeding to evaluate the number of cells added.

2. Establishing the 3D stromal-endothelial cell co-culture

1. Prepare the GFP-HUVEC cell suspension.
 1. Prepare flasks for the HUVEC culture by coating with a solution consisting of 150 μ g/mL rat-tail collagen I in 0.02 M acetic acid for 30 min at 37 °C. Rinse once with PBS before use.
 2. Grow the GFP-HUVECs to a confluence level of 80%-100% in EGM-2 supplemented with 10% FBS in an incubator at 37 °C and 5% CO₂ in a humidified atmosphere. The cells may be used up to passage 7.
 3. Wash the cells with PBS, and detach them using 0.05% Trypsin-EDTA for 2-3 min at 37 °C. Stop

the detachment process by flushing with basal medium (MEM α supplemented with 10% FBS and 1% penicillin-streptomycin). Collect the suspended cells in a 50 mL conical centrifuge tube.

4. Count the cells using a hemacytometer or an automated cell counter, and determine the total number of cells present in the suspension.
 5. Pellet the cells by centrifugation at 200 x g for 5 min. Carefully remove the supernatant.
 6. Resuspend the cells in an appropriate volume of basal medium to achieve a concentration of 1×10^7 cells/mL of stock solution.
 7. Prepare 50 mL conical centrifuge tubes containing the required volume of basal medium supplemented with the respective growth factors (FGF-2 and BMP-2 at defined concentrations, e.g., 0 ng/mL, 25 ng/mL, 50 ng/mL, 100 ng/mL, or 200 ng/mL) as described for the hBM-MSCs in step 1.1.6.
 8. Add the GFP-HUVECs from the stock solution at a dilution of 1:66.67 to achieve a concentration of 1.5×10^5 cells/mL, as described for the hBM-MSCs in step 1.1.7.
2. Aspirate the medium from the plate containing the stromal monoculture, as described for the buffer removal in step 1.2.2.
 3. Add 200 μ L/well of the GFP-HUVEC cell suspension prepared in step 2.1.8 as described for the hBM-MSC addition in step 1.3.
 4. Incubate at 37 °C and 5% CO₂ in a humidified atmosphere. Change the medium every 3-4 days.
 5. Monitor the development of the culture by bright-field and fluorescence microscopy using a 5x objective as desired.

Maintain the cultures until day 4 or day 7 of co-culture for early or intermediate characterizations, respectively, or as desired.

3. Characterization procedure 1: Quantifying endothelial cell network formation

1. At the desired time points, acquire the GFP signal from the GFP-HUVECs with fluorescence microscopy using settings suitable for quantification (i.e., best focus, high contrast, and low magnification [e.g., 5x] for larger fields of view).
2. Pre-process equally all the images acquired on the same day (e.g., using Fiji³²) to further enhance the contrast. Note that the GFP signal may become dimmer with culture time; therefore, images acquired on different days may need different processing.
 1. If using Fiji or ImageJ, open all the GFP channel images of the same time point, and open the **Brightness & Contrast** menu. Select an image that represents an intermediate condition (not the dimmest and not the brightest signal), and auto-adjust the contrast by selecting **Auto**. Select **Set**, and check **Propagate to all Other Open Images**.
 2. Visually assess whether the range automatically selected fits all the images of the current time point, and manually re-adjust and re-propagate to all the images as needed.
 3. Save the adjusted images as TIF files, and repeat step 3.2.1 and step 3.2.2 for the other time points acquired.
3. Apply a median blur filter (e.g., radius 3 for 2048x2048 images) to all the images to avoid artifact recognition downstream and, thus, facilitate accurate

network identification. Reduce the size by binning (2x2) and save all pre-processed images as grayscale RGB Color TIF files in a folder for quantification. These steps can be done manually or in batch mode using macros that the authors will share upon request.

4. Analyze all the images in the folder created in steps 3.1-3.3 using the **Batch Process** mode in the **Angiogenesis Analyzer** for ImageJ³³. Note that depending on the size of the images and available working memory, this may take a few minutes per image.
5. Validate the quantification results by examining the overlays of the recognized structures and the original images. If the algorithm recognizes artificial structures, where only a few or no cells can be seen in the original image, adjust the pre-processing parameters, and re-analyze the original images, or exclude such problematic areas and/or replicate images from the analysis.
6. Normalize the obtained values to an area of 1 mm² by multiplying the values of each sample by the ratio of the analyzed area to 1 mm². This step is of particular importance if images of different sizes are used.
7. Extract various network parameters, such as the total network length, number of junctions, number of segments, number of isolated segments, branching interval, and mean mesh size, from the analysis, and use them to characterize the endothelial network at different time points and under different culture conditions.

4. Characterization procedure 2: Assessing ECM deposition

1. At the desired end time points, assess ECM deposition using immunofluorescence. Add primary antibodies against various ECM molecules in 100 μ L of the culture

medium during the last 6 h of culture or after fixation, as described below.

1. Wash the cultures once with 200 μ L/well of PBS for 5 min at RT, and fix them with 100 μ L/well of 4% paraformaldehyde under a chemical fume hood for 30 min at RT. Note that it is advised to fix all the wells of a plate at the same time, as the surrounding cultures may be damaged during this step. Wash the fixed cultures with 200 μ L/well of PBS at RT three times for 5 min each time, and store at 4 °C in 200 μ L/well of PBS, or proceed immediately to the next step.
2. Before incubating with primary antibodies against ECM molecules after fixation, incubate the fixed cultures with 200 μ L/well of 1% BSA in PBS as a blocking solution for 30 min at RT.
 1. Aspirate the blocking solution, and incubate with 100 μ L/well of the primary antibody solution in 1% BSA in PBS overnight at 4 °C. Wash with 200 μ L/well of PBS three times for 5 min, at least 3 h, and 5 min, respectively, at RT.

NOTE: The long washing step is required for the complete diffusion of the unbound antibody out of the hydrogel.
3. To facilitate the penetration of the secondary staining solution, including intracellular counterstains, permeabilize the cultures using 0.3% Triton X-100 and 1% BSA in PBS for 30-90 min at RT, depending on the cellular density of the cultures.

NOTE: For the antibody-based staining of intracellular molecules, this step should be performed before the incubation with the primary antibody described in step 4.1.2.

4. Prepare secondary staining solutions containing the respective secondary antibodies and counterstains as desired (e.g., a nuclear stain such as DAPI and a cytoskeletal stain such as phalloidin-rhodamine).
 1. Prepare a staining buffer consisting of 0.1% Triton X-100, 1% BSA in PBS, and counterstains (e.g., 1 µg/mL DAPI and 1:4,000 phalloidin-rhodamine), and add the respective secondary antibodies at the recommended dilutions.
 2. Add 100 µL/well of secondary staining solution, and incubate overnight at 4 °C. Similar to the procedure after the primary antibody incubation, wash with 200 µL/well of PBS three times for 5 min, at least 3 h, and 5 min, respectively, at RT.
 5. For the 3D resolving of the structures, acquire confocal stacks starting at the glass bottom with a z-step of 2.5 µm reaching a final height of 500 µm, use a 10x objective, and a 0.75x digital zoom. To generate a 3D reconstruction of the GFP and F-actin signal in Fiji, threshold each channel separately before creating a composite and generating the reconstruction using Fiji 3D Viewer.
 6. For the visualization of the deposited ECM from the immunostainings, acquire confocal stacks of a height of 100 µm with a z-step of 5 µm, a 10x objective, and a 1.5x digital zoom. Generate maximum intensity projections, and adjust the brightness and contrast for each channel separately in Fiji before creating a composite.
2. Perform direct color stainings of the extracellular environment.
 1. Add 200 µL/well of Picrosirius Red staining solution to the paraformaldehyde-fixed wells, and incubate for 1 h at RT.
 2. Next, wash the stained wells five times with distilled water, followed by washing twice every day or every second day for 3-4 days while monitoring the sample color clearing. Keep the plates at 4 °C during the long washing steps (i.e., anything exceeding 6 h).
 3. Acquire images of the stained samples using a bright-field microscope equipped with a color camera, and maintain an equal white balance across the conditions. To acquire overviews of the samples, use a low magnification (e.g., 2.5x) to scan the entire well. If the microscope does not come with software supporting automated stitching, do it manually (e.g., using Pairwise Stitching in Fiji³⁴).

NOTE: The wells previously used for immunofluorescence can be used for this, provided that fluorescence image acquisition is completed.
 4. Follow the same steps described for Picrosirius Red staining in steps 4.2.1-4.2.3 to perform Alizarin Red staining, washing, and imaging.

5. Characterization procedure 3: Assessing osteogenic differentiation by monitoring ALP activity

1. At different culture end time points (e.g., day 4 and day 7 of co-culture), quantitatively assess ALP activity by using 5-bromo-4-chloro-3-indolyl phosphate (BCIP)/nitro blue tetrazolium (NBT) staining.
 1. Wash the cultures once with 200 µL/well of PBS before incubating with the BCIP/NBT substrate solution, which should be prepared following the

manufacturer's instructions. Incubate at 37 °C while periodically monitoring color development. Once the color starts to develop in non-osteogenic conditions, immediately wash once with 200 µL/well of PBS before fixing with 4% paraformaldehyde, as described in step 4.1.1.

2. Acquire color images of the stained samples, as described in step 4.2.3 for Picrosirius Red staining.
2. At different culture end time points (e.g., day 4 and day 7 of co-culture), quantify the ALP activity in the cell lysates.
 1. Wash the cultures three times with 200 µL/well of PBS before incubating with 200 µL/well of 0.25% Trypsin-EDTA at 37 °C. Every 10 min, agitate the cultures by vigorously pipetting up and down to facilitate digestion, and monitor the culture morphology with a standard cell culture microscope.
 2. Once a liquid, single-cell suspension with no elongated cellular structures in the wells is obtained (typically after 20-30 min), transfer the samples to 2 mL tubes, add 200 µL of MSC basal medium to inhibit the Trypsin, and centrifuge at 500 x g for 5 min to pellet the retrieved cells. Decant the supernatant, and freeze the pellets at -80 °C, or proceed directly to step 5.2.3.
 3. Thaw the cell pellets obtained in step 5.2.2, and incubate with 500 µL of lysis buffer consisting of 0.56 M 2-Amino-2-methyl-1-propanol, 0.2% Triton X-100, pH 10, for 30 min on ice. Next, centrifuge at 16,100 x g for 10 min at 4 °C, and keep the samples on ice. After the measurements described in step 5.2.7, freeze the samples at -20 °C or -80 °C, or directly continue with the DNA quantification, as described in step 5.2.8.

NOTE: The lysis buffer can be prepared in advance, sterile-filtered, and stored at 4 °C.

4. Prepare the ALP reagent consisting of 20 mM 4-Nitrophenyl phosphate disodium salt hexahydrate and 4 mM MgCl₂ in lysis buffer.

NOTE: It is best to prepare this solution fresh on the day of quantification.
5. Without disturbing any pelleted debris, dispense 50 µL of the cell lysate supernatant prepared in step 5.2.3 into the wells of a standard, transparent, tissue-culture 96-well plate in duplicates. Add lysis buffer to two wells as blank controls.
6. With a multichannel pipette, add 50 µL/well of ALP reagent to the wells filled in step 5.2.5. Briefly shake the plate, and incubate at 37 °C for 10 min protected from light. Wells with higher ALP activity will appear yellow. Stop the reaction by adding 100 µL/well of 1 M NaOH using a multichannel pipette.
7. Read the optical density at 410 nm using a plate reader. Average the technical duplicates, and subtract the average of the blank controls.
8. Perform DNA quantification to normalize the ALP activity determined in the previous steps against the total cell number. Here, a method based on fluorescence measurements is described, but any other method for DNA quantification in cell lysates is compatible with the assay. Prepare the reagents and DNA standards required for DNA quantification using commercially available kits according to the manufacturers' instructions.

NOTE: It is recommended to use lysis buffer for preparing the DNA standards.

9. If the samples used for ALP quantification described in step 5.2.3 were frozen, thaw them, centrifuge at 16,100 x g for 2 min at 4 °C, and place them on ice. Without disturbing any pelleted debris, dispense 50 µL of the cell lysate supernatant into the wells of a black 96-well plate in duplicates. Freeze the samples at -20 °C or -80 °C, and repeat the ALP and DNA quantifications if necessary. Add the DNA standards in duplicates.
10. With a multichannel pipette, add 50 µL of the DNA staining agent, incubate, and read the fluorescence intensity as per manufacturer's instructions. Using the standard curve values, determine and apply the conversion of the measured intensity values to the DNA concentrations.
11. Normalize the ALP values obtained in step 5.2.7 by dividing them by the respective DNA concentration of each sample.

6. Application 1: Performing drug sensitivity assays

1. When the endothelial networks are fully developed (typically at day 4 of the stromal-endothelial cell co-cultures), add anti-angiogenic compounds, such as bevacizumab, to the cultures in fresh culture medium, and test their activity over time and under different conditions (e.g., different concentrations of FGF-2 or BMP-2).
 1. Prepare fresh culture medium containing the same growth factors used for the respective cultures until that point.
 1. Prepare a control solution consisting of the diluent of the compound of interest (e.g., for

bevacizumab: 60 mg/mL α-trehalose dihydrate, 0.4 mg/mL Tween20, 5.8 mg/mL sodium phosphate, monobasic and monohydrate, and 1.2 mg/mL sodium phosphate dibasic, anhydrous), and sterile-filter it.

2. Add the compound of interest at the desired concentration (e.g., 10 µg/mL bevacizumab) and an equal volume of the control solution to the culture medium designated for the test and control conditions, respectively.
2. Aspirate the medium from the culture, and add 200 µL/well of the medium freshly prepared in step 6.1.1. Incubate for a time appropriate for the compound to be tested (e.g., for bevacizumab: 2 days). Monitor the culture development, and characterize the endothelial networks as described in section 3. Assess the effectiveness of the compound in inhibiting angiogenesis or ablating the pre-formed structures using the GFP images and the quantitative network parameters extracted from the analysis described in step 3.7.

7. Application 2: Establishing advanced co-culture systems with various cancer cell types

1. At day 4 of co-culture, when the endothelial networks are mostly established, add other cell types, such as MDA-MB-231 or U2OS cancer cells, to the cultures in fresh culture medium.
 1. Label the cancer cells using a cell-compatible live dye as per the manufacturer's instructions in order to be able to distinguish them from the GFP-labeled HUVECs and non-labeled hBM-MSCs in the co-cultures.

2. Prepare a suspension of cancer cells at a concentration of 1.5×10^4 cells/mL in fresh culture medium containing the same growth factors used for the respective cultures until that point.
2. Monitor the culture development and cancer cell localization as desired.

NOTE: Depending on cancer type, activity, and environment, it might take a few days for them to reach the vascular structures in the stromal-endothelial cell co-cultures (e.g., 2 days for MDA-BM-231 and U2OS). Therefore, the time-lapse imaging to visualize the cancer-vascular cell interactions should be timed accordingly.

Representative Results

Vascular niche cultures were established by sequentially seeding hBM-MSCs and GFP-HUVECs onto pre-cast PEG-based hydrogels with a stiffness gradient within a 96-well imaging plate (**Figure 1**). The cultures were monitored longitudinally via live epifluorescence microscopy and further characterized at selected time points. The extracellular compartment was assessed via direct color stainings and antibody-based stainings. ALP activity was quantified after retrieving and lysing the cells from the generated niches. Furthermore, we demonstrate the suitability of this platform for anti-angiogenic drug sensitivity assays and as a basis for cancer co-culture models.

Co-cultures of hBM-MSCs and GFP-expressing HUVECs were established by seeding 3×10^4 cells/well in the absence of growth factors or in the presence of either FGF-2 or BMP-2 at 50 ng/mL, as described in the protocol. From an early time point, differences between the cultures could be observed both from the bright-field and fluorescence

images showing only the GFP-HUVECs (**Figure 2A**). By observing the same areas longitudinally, differences in the development of the cultures could be noted, such as a faster development in the presence of FGF-2. Generally, the cultures appeared less developed in the absence of any growth factor, with fewer cells of either type spreading and the presence of acellular areas. In contrast, the bright-field images showed the most dense cultures in the presence of BMP-2. However, vascular-like networks formed in both growth factor-containing conditions, and the most extensive and interconnected networks were formed with FGF-2. These observed differences could also be quantified using **Angiogenesis Analyzer** for ImageJ. Indeed, the total network length was highest in the presence of FGF-2 and lowest in the absence of growth factors (**Figure 2B**). The number of junctions indicating branching points in the networks followed the same trend as the total length (**Figure 2C**). Conversely, both growth factor-containing conditions featured significantly fewer isolated segments, indicating higher interconnectivity, than the condition without any growth factor (**Figure 2D**). Additionally, 3D confocal imaging revealed stronger endothelial cell penetration in terms of depth in the FGF-2-stimulated condition (**Figure 2E**).

hBM-MSC/GFP-HUVEC co-cultures were maintained for 7 days in the presence of FGF-2 or BMP-2 before being fixed and stained for ECM components. Immunocytochemical stainings followed by confocal laser scanning microscopy showed striking differences in culture morphology depending on the type of growth factor supplementation (**Figure 3A**). With FGF-2, the culture was organized into condensed microvascular-like structures, which were dense in both endothelial and mesenchymal cells, whereas in the presence of BMP-2, the hBM-MSCs spanned a much larger area, as evident from the more extensive F-actin-positive and GFP-

negative areas. The ECM proteins fibronectin and collagen I were localized in a similar manner, while laminin and collagen IV were more concentrated around the endothelial structures. However, this increased concentration around the endothelial structures was much more pronounced in the presence of FGF-2 than in the presence of BMP-2. In addition to the antibody-based stainings, direct color stainings were performed to assess the overall fibrotic state of the ECM (Picrosirius Red staining; **Figure 3B**), as well as the deposition of Ca on the ECM (Alizarin Red staining; **Figure 3C**) of the formed niches. The Picrosirius Red staining was stronger and more extensive in the niches cultured with BMP-2, and the Alizarin Red staining followed the same trend.

Next, the cultures were characterized in terms of their osteogenic potential by assessing ALP activity as an early osteogenic marker. On day 4 and day 7 of co-culture, cells were retrieved from the niches by digesting the hydrogels with Trypsin. To quantify the ALP activity, the retrieved cells were lysed, and a pNPP assay was performed. The values obtained were normalized against the total DNA for each sample to account for potential differences in the cell numbers across conditions. Indeed, small differences between the DNA content of the conditions could be observed, and the fewest cells were retrieved from the condition without any growth factor (not shown). The normalized ALP activity, however, varied greatly across conditions, with a trend of increasing activity with higher concentrations of BMP-2 and a plateau at 100 ng/mL (**Figure 4A,B**). The lowest activity levels were identified for the condition containing 50 ng/mL FGF-2. While similar trends could be observed for both of the time points assessed, all the values significantly increased over time in culture from day 4 to day 7. In addition to the quantitative assay, the ALP activity could be qualitatively visualized using direct color staining based on the BCIP/

NBT substrate conversion. More extensive and more intense purple staining was observed in the presence of BMP-2 as compared to FGF-2 (**Figure 4C**).

To demonstrate two potential applications of the characterized osteogenic niches, a proof-of-concept drug sensitivity study and cancer co-cultures were performed. For the drug sensitivity assay, bevacizumab or a control solution consisting of the diluent of the bevacizumab formulation was added to the culture medium containing fresh BMP-2. On day 4, when established networks were formed in the presence of 50 ng/mL BMP-2, either the control solution or bevacizumab-containing medium was added during the regular medium change, and the cultures were monitored using fluorescence imaging. The addition of 10 µg/mL bevacizumab led to the retraction or ablation of the previously formed network, while the control condition still featured extensive networks 2 days after the medium change (**Figure 5A,B**). These changes could also be quantified by tracking the total length of the networks using **Angiogenesis Analyzer** for ImageJ on fluorescence images acquired daily (**Figure 5C**). Alternatively, bevacizumab or any other compound could also be added from the beginning of the co-culture to assess their influence on the formation of the networks. In the case of bevacizumab, this completely inhibited the formation of endothelial networks (not shown).

For the second application, MDA-MB-231 breast cancer or U2OS osteosarcoma cells were added to day 4 co-cultures at a density of 1.5×10^3 cells/well in fresh culture medium containing 50 ng/mL BMP-2. To distinguish them from the GFP-labelled HUVECs and the non-labeled hBM-MSCs, the cancer cells were incubated with CellTrace FarRed just before the seeding onto the osteogenic niches. The cultures were monitored by fluorescence microscopy; at the

beginning, most of the cancer cells localized near the surface of the substrate, but after 2 days, they could be found in closer proximity to the layers containing the vascular co-cultures. Thus, day 2 was selected as the starting point for time-lapse microscopy to show the dynamics of the interactions between the cancer cells and the cells within the vascular niche. Interestingly, the MDA-MB-231 cells could be

seen both approaching and moving away from endothelial structures and, thus, were possibly probing or remodeling their environment (**Figure 5D**). Using CellTrace FarRed as a label for the cancer cells, GFP as a label for HUVECs, and additional staining for F-actin, all the cell types could be distinguished using confocal laser scanning microscopy (**Figure 5E**).

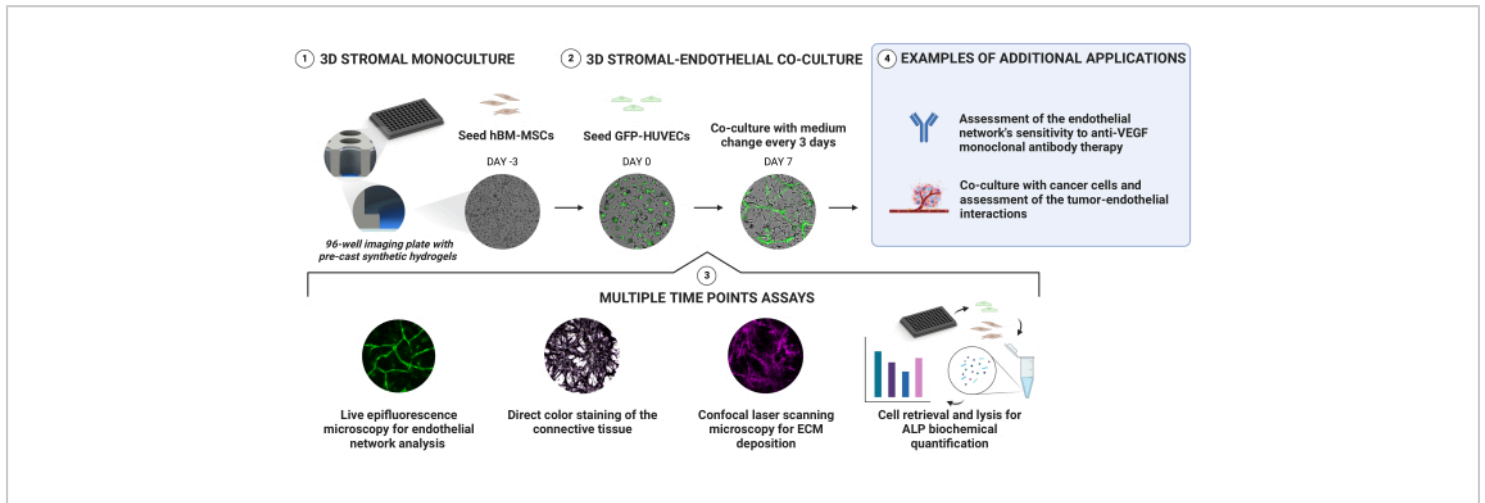


Figure 1: A simple approach for the reliable generation of vascularized, osteogenic niches. Pre-cast synthetic hydrogels with an in-depth stiffness gradient allow for the generation of 3D cultures via sequential cell seeding without the need for direct encapsulation. hBM-MSCs are pre-cultured for 3 days before GFP-expressing HUVECs are added. The cultures are monitored by acquiring bright-field and GFP signals longitudinally. At select time points, the niches are further evaluated for their ECM deposition and osteogenic state. Alkaline phosphatase activity is assessed via direct color staining and by retrieving cells from the niches and performing a pNPP assay on the cell lysates. [Please click here to view a larger version of this figure.](#)

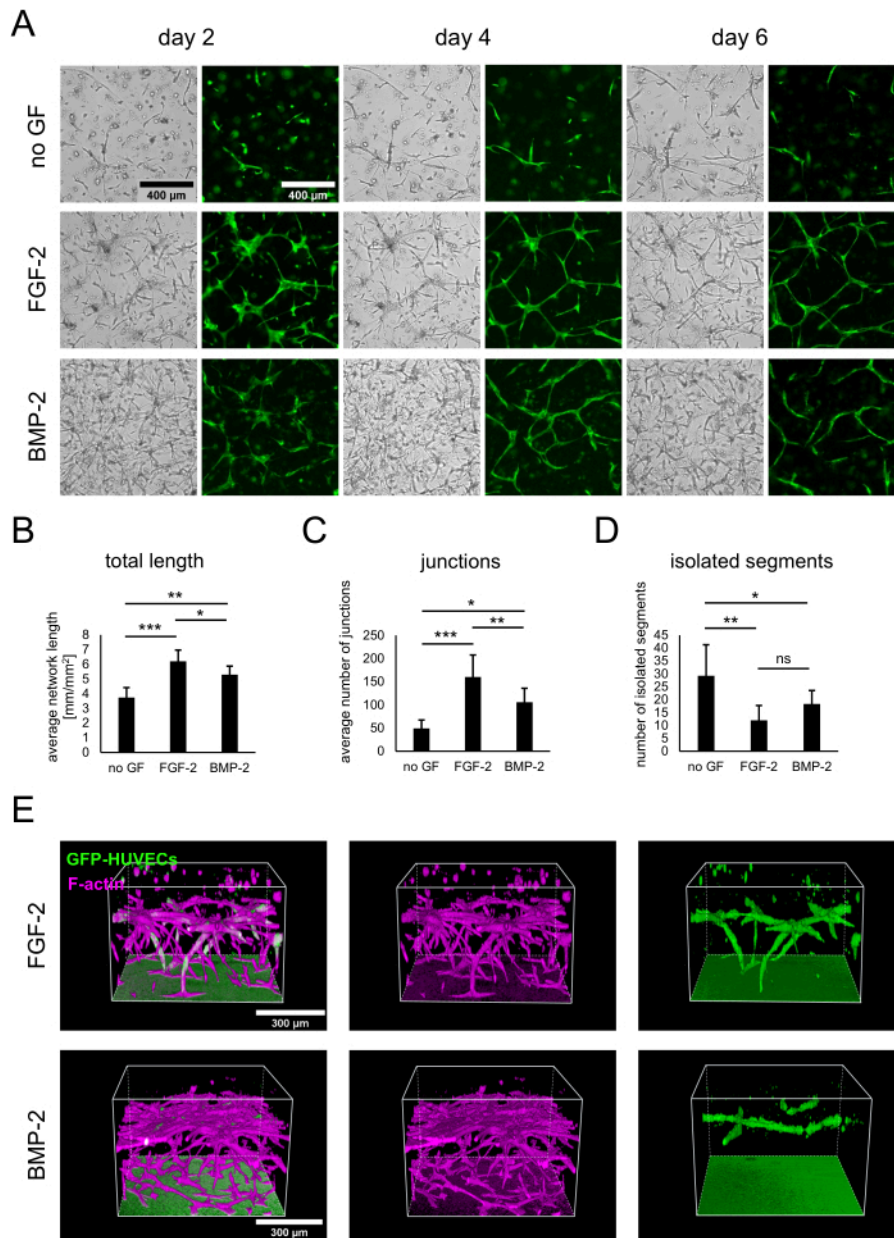


Figure 2: Stimulation of vascular-like networks with FGF-2 or BMP-2. (A) Bright-field and fluorescence (GFP) images were acquired on day 2, day 4, and day 6 of the co-culture of cells grown in the absence of growth factors or in the presence of FGF-2 or BMP-2, both at 50 ng/mL. Scale bar: 400 μ m. (B-D) Quantified parameters of the GFP-HUVEC-networks imaged on day 4 of co-culture, analyzed using **Angiogenesis Analyzer** for ImageJ. The data are represented as mean \pm standard deviation. The statistical analysis was performed using GraphPad Prism 9.5.1. An ordinary one-way ANOVA with Dunnett's multiple comparisons test was performed with $n \geq 4$; * $P < 0.05$; ** $P < 0.01$; *** $P < 0.001$. (E) Three-dimensional reconstructions generated from confocal stacks (total height: 547.5 μ m; z-step: 2.5 μ m) of the GFP and F-actin signals for

the FGF-2- (top row) and BMP-2- (bottom row) stimulated conditions. Scale bar: 300 μm . [Please click here to view a larger version of this figure.](#)

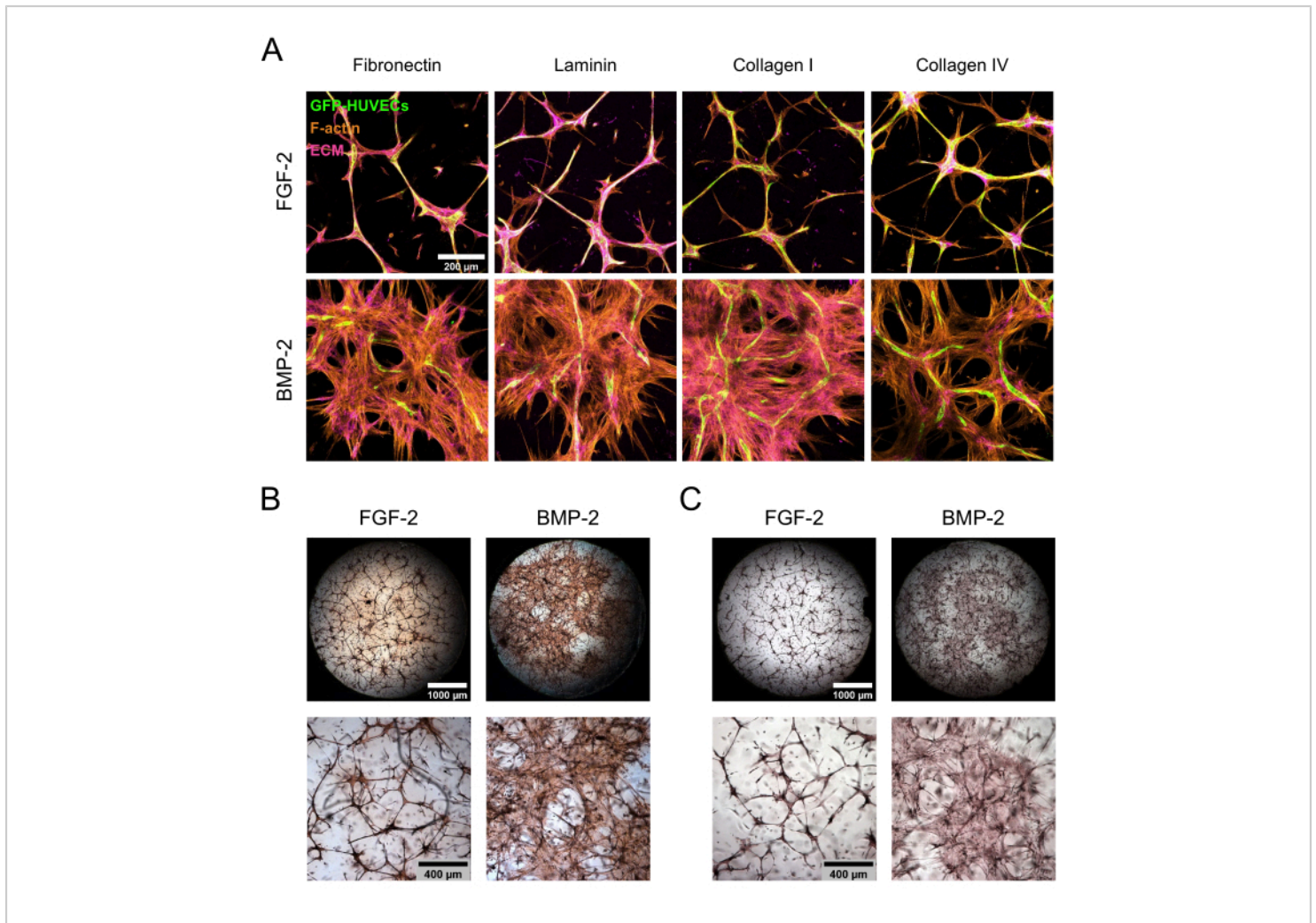


Figure 3: Induction of de-localized hBM-MSC spreading and ECM deposition by BMP-2. (A-C) The 7 day co-cultures grown in the presence of either FGF-2 or BMP-2 were subjected to (A) immunofluorescence or (B,C) direct color staining. (A) The cultures were stained for F-actin and the ECM proteins fibronectin, laminin, collagen I, and collagen IV. The images depict the maximum intensity projections of the confocal stacks (total height: 100 μm ; z-step: 5 μm). Scale bar: 200 μm . (B,C) The cultures were stained using (B) Picosirius Red and (C) Alizarin Red. The top row depicts stitched, whole-well overviews of the images acquired at 2.5x magnification (scale bar: 1,000 μm), while the bottom row depicts one field of view acquired at 5x magnification (scale bar: 400 μm). [Please click here to view a larger version of this figure.](#)

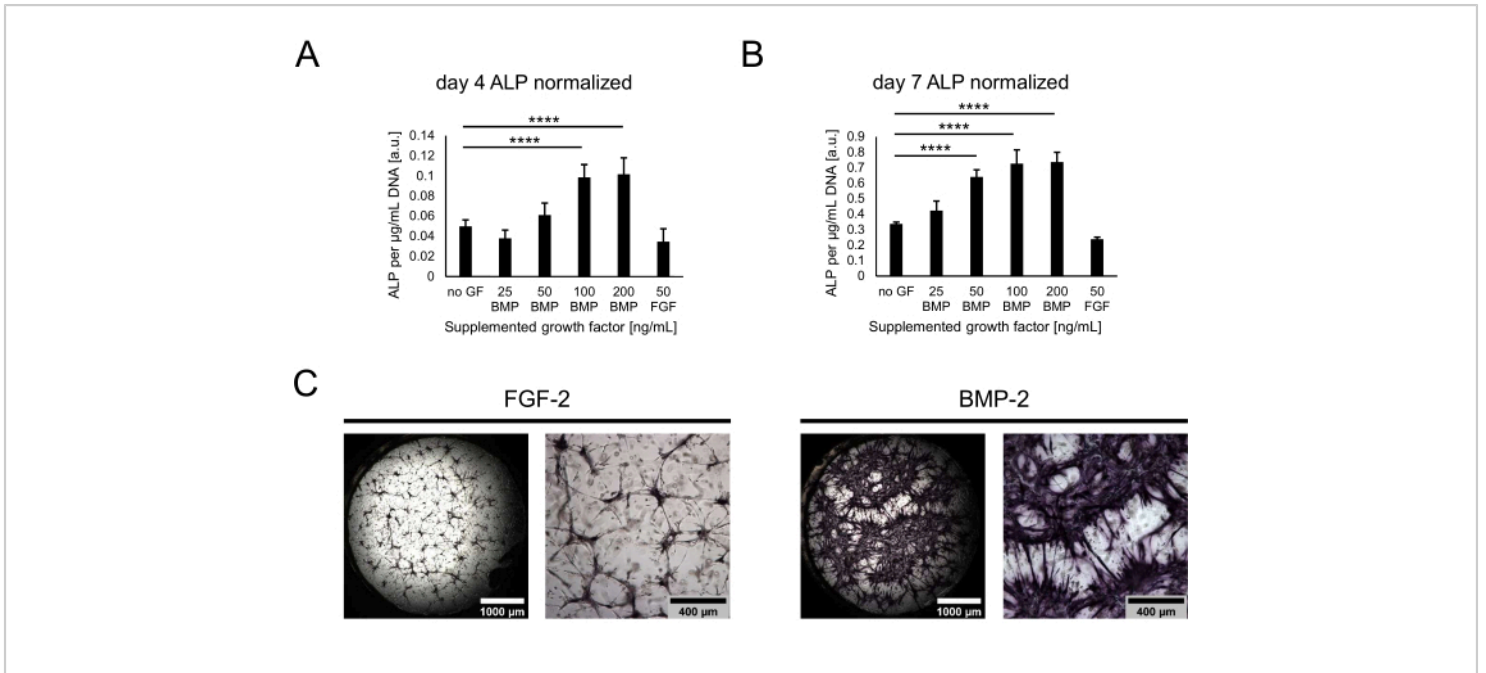


Figure 4: Biochemical assessment of BMP-2-induced ALP activity through direct color staining. (A,B) The ALP activity was determined in the cell lysates of cultures grown in the absence of growth factors or in the presence of BMP-2 at different concentrations or FGF-2 at 50 ng/mL for (A) 4 days or (B) 7 days of co-culture. The ALP activity is shown normalized to the DNA content of each lysate sample. The data are represented as mean \pm standard deviation. The statistical analysis was performed using GraphPad Prism 9.5.1. An ordinary one-way ANOVA with Dunnett's multiple comparisons test was performed with $n = 5$; **** $P < 0.0001$. (C) Direct color staining of the ALP activity in niches grown in the presence of 50 ng/mL FGF-2 or BMP-2 for 7 days of co-culture. The images on the left-hand side depict stitched whole-well overviews of images acquired at 2.5x magnification (scale bar: 1,000 μm), while the images on the right-hand side depict one field of view acquired at 5x magnification (scale bar: 400 μm). [Please click here to view a larger version of this figure.](#)

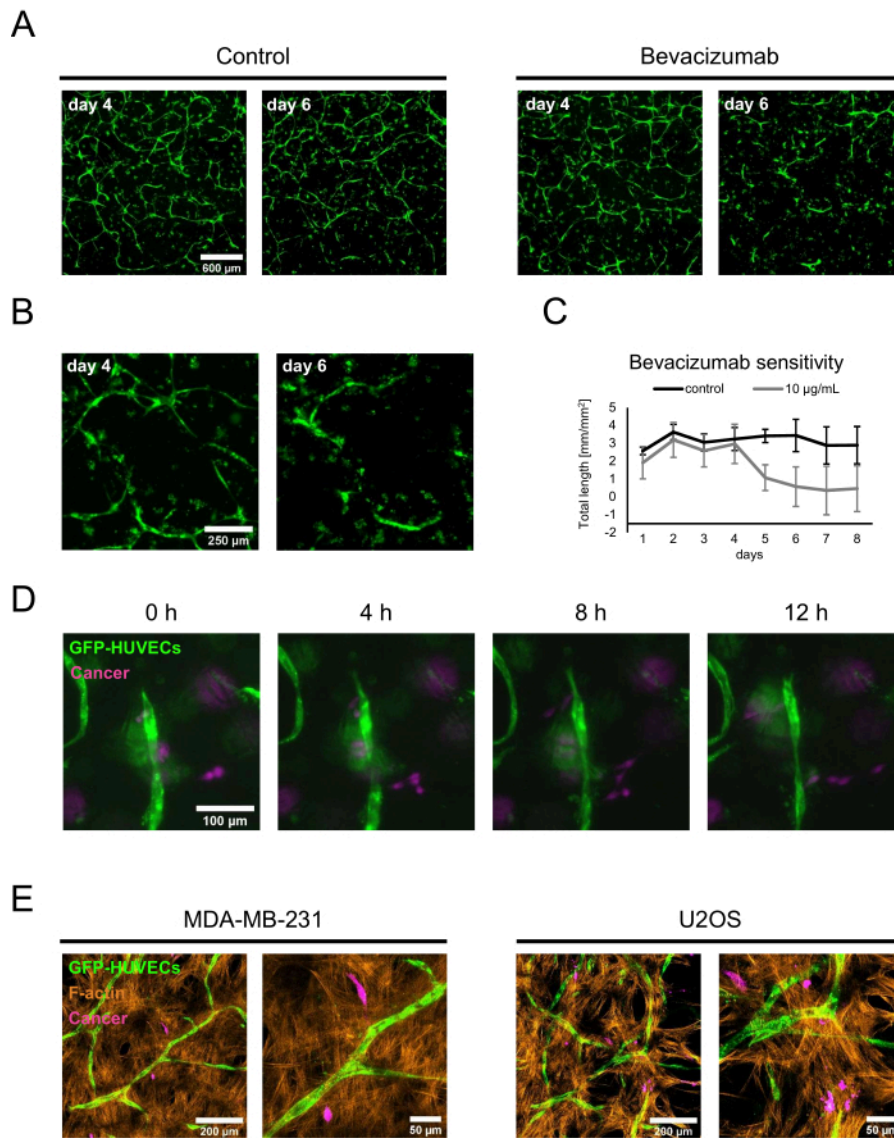


Figure 5: Employment of osteogenic, vascularized niches in advanced cancer models. (A) The GFP signals of cultures grown in the presence of BMP-2 were imaged on day 4 of co-culture before a control solution (left) or bevacizumab at 10 $\mu\text{g/mL}$ (right) were added for 2 days, after which the cultures were imaged again (day 6 of co-culture). Scale bar: 600 μm . (B) Higher magnification images of the bevacizumab-treated cultures are shown in A. Scale bar: 250 μm . (C) The total length of the endothelial networks as shown in A were quantified using **Angiogenesis Analyzer** for ImageJ from images acquired daily; $n \geq 3$. (D) CellTrace FarRed-labeled MDA-MB-231 breast cancer cells were added to the 4 day co-cultures grown in the presence of BMP-2, and time-lapse images were acquired starting 2 days after the cancer cell addition. Scale bar: 100 μm . (E) Maximum intensity projections of confocal stacks (total height: 70 μm ; z-step: 2.4 μm) of triple co-cultures generated as described in D and fixed and stained for F-actin. Left: niches featuring MDA-MB-231 breast cancer cells; right: niches

featuring U2OS osteosarcoma cells. Scale bars for images on the left: 200 μm ; scale bars for images on the right: 50 μm .

[Please click here to view a larger version of this figure.](#)

Discussion

Here, we describe a protocol for the establishment of an *in vitro* model of highly vascularized bone and bone marrow niches in a fully synthetic and controllable 3D PEG-based matrix, which has a variety of applications in bone and bone marrow biology research, tissue engineering, and cancer research. This model builds on a synthetic PEG-based hydrogel that is functionalized with RGD peptides and MMP cleavage sites and is cast with an in-depth density gradient on glass-bottom 96-well imaging plates³⁰. This plug-and-play platform was shown to allow the establishment of highly interconnected 3D cellular networks without the need to encapsulate cells into the hydrogel. Similar to the earlier-described cell encapsulation protocol, in this work, we show the remodeling of the substrate by a cell-inherent ECM²⁸ to create a cell type-specific microenvironment. Thus, with this method, drug screening assays and high-content analyses can be easily performed under highly reproducible, organotypic 3D culture conditions. The glass-bottom 96-well plates and the optically transparent hydrogels render the platform compatible with liquid handling automation and high-throughput microscopy.

The first step in generating an osteogenic vascular bone marrow niche is the pre-culture of hBM-MSCs on the PEG hydrogel for at least 3 days. During this time, they attach to the hydrogel, penetrate it, and start establishing cell-cell contacts and ECM deposition. Before seeding the hBM-MSCs, the storage buffer must be removed. As the hydrogel is situated inside an inner well within the standard well of the 96-well imaging plate, it is safe to insert the aspiration tip along the side of the well until it touches the inner well ring. A

vacuum pump can be used for aspiration if it is set at the lowest possible suction force. Alternatively, an automated plate washer with the nozzle height adjusted to at least 0.8 mm above the inner well ring can be used to aspirate the buffer from the hydrogel plate. Using automation for liquid handling can minimize damage to the hydrogel surface and lead to higher reproducibility of the resulting cultures. Small defects on the hydrogel surface become visible once the cells settle on the hydrogel and appear on a lower focus plane in defective hydrogel areas. Therefore, acquiring reference images on day 0 serves as a good quality control for the cell seeding homogeneity and hydrogel surface integrity. While small hydrogel surface defects do not preclude the further use of the well, the cells tend to cluster on the defective areas and may grow into non-representative patterns or more quickly reach the bottom glass, where they grow into a monolayer. These artifacts must be noted when using/evaluating these wells. Similar considerations apply for any medium changes performed during the entire duration of the assay.

The second step of the protocol involves the addition of GFP-HUVECs to the pre-formed hBM-MSC monoculture (day 0 of co-culture). The ECM deposited by the hBM-MSC provides a great scaffold for the growth of endothelial cells, which in this work, even in the presence of hBM-MSC-conditioned medium, could only form round cell clusters on the hydrogels (not shown). Upon seeding on the hBM-MSC cultures, the HUVECs integrate and form microvessel-like structures comparable to the ones observed in co-cultures generated by cell encapsulation^{27,28}. Typically, well-developed 3D microvascular-like networks form within 4 days of co-culture, and this can be longitudinally monitored by the use of

GFP-labeled HUVECs. These structures can be maintained for at least 7 days in culture, meaning there is sufficient time to follow changes in the vascular network organization in response to treatments, such as for the screening of anti-angiogenic drugs. The morphological elements of the endothelial network can be quantified in batch mode by segmenting the GFP images using well-established tools, such as the **Angiogenesis Analyzer** plugin of ImageJ³³, and their parameters can be used to evaluate, for example, drug efficacy and pharmacodynamics.

One significant advantage of the described cellular model for many potential applications is its plasticity. Simply supplementing the culture medium with different growth factors can change the appearance of the co-culture. For example, the presence of BMP-2 throughout the mono- and co-culture period creates an osteogenic vascular niche, showing increased ALP activity, extracellular calcium deposition, as well as ECM assembly and deposition. On the contrary, in the presence of FGF-2, the osteogenic markers are absent, and the co-culture forms fewer lateral cell associations but shows more pronounced 3D cell growth. The fact that FGF-2 suppresses ALP activity while BMP-2 elicits stronger ALP activity compared to no growth factor treatment is in accordance with previous observations²⁷. Yet, despite these big differences in the hBM-MSC stromal component, the extent of the microvascular network was very similar for the two growth factor-treated conditions in this work. In the control cultures, only a few short vascular networks formed, representing perhaps a poorly vascularized bone marrow niche. This suggests that by simply changing the type, concentration, and timing of the growth factors added to the culture medium, a range of well-defined vascularized bone marrow niches, as would be required for comparative studies, could be produced. However, to ensure reproducible

results, it is important to note that the culture progression and morphology may vary depending on the history of the cells used (e.g., the passage number and detachment method used during routine culture maintenance), and it is advisable to control for such factors during the assay design.

Here, as a first application of this model, we demonstrate the sensitivity of the engineered microvascular networks to treatment with 10 µg/mL bevacizumab. Notably, it is important to confirm that the algorithm used can accurately recognize the endothelial network, as artifacts are often generated in images with poorly developed networks. If this is the case, the parameters used for image processing (before and during segmentation) need to be fine-tuned, often on a trial-and-error basis.

As a second application, we present an advanced co-culture model formed by the sequential seeding of mesenchymal, endothelial, and cancer cells. This model allows for studying the interactions between cancer cells, the stroma, and the vasculature of the bone marrow, which may be important factors during metastasis. Additionally, this model could be used for drug screening applications and testing compounds with targets beyond angiogenesis.

In 2D cultures, cells do not receive physiologic microenvironmental signals, do not acquire naturally occurring cell morphologies, and consequently, differentiate differently compared to cells in native 3D environments³⁵. When grown in engineered 3D hydrogels, the cells deposit an inherent ECM early on, which provides adhesion sites and can be actively remodeled^{28,36}. Here, to establish a simplified 3D model for screening applications, vessel-forming cells were seeded onto the surface of engineered hydrogels and allowed to establish vascular networks in the absence of perfusion. The imaging-based evaluations

were conducted on 2D projections of the endothelial cells contributing to vascular structures. However, only confocal images revealed the less pronounced ingrowth of the 3D vascular networks in the BMP-2-stimulated samples when compared to the FGF-2-stimulated samples. This suggests that the length of the formed vascular structures was underestimated, while their connectivity was overestimated. Additionally, interactions between perivascular and endothelial cells and vascular lumen formation have not been investigated. These aspects, especially in terms of drug treatment responses, will require further attention. Finally, refined protocols to first establish extensive 3D vascular networks and only then induce their osteogenic differentiation would be desirable to generate more physiological bone and bone marrow models.

Overall, the model presented here is highly versatile and can be easily tailored toward specific applications. For example, mesenchymal and endothelial cells from different sources could be used. It is known that adipose tissue MSCs and umbilical cord MSCs express different angiogenic factors compared to BM-MSCs, and they can easily be substituted as an alternative stromal component³⁷. Endothelial cells isolated from already defined bone marrow niches could also be used instead of HUVECs. One could also establish the co-culture with patient-derived, matching bone marrow mesenchymal and endothelial cells for personalized medicine applications, as has recently been suggested for vascularized muscle co-cultures³⁸. Additionally, the design of the hydrogel plate allows the longitudinal monitoring of the culture with both bright-field and fluorescence microscopy, thus offering the user the possibility to shorten or extend the culture time depending on the application. Alternatively, the cell densities used for seeding could be adjusted accordingly to accelerate or delay the formation of the cell network if shorter or longer

observation times are needed than those in this protocol. In any case, caution is needed to avoid cell overgrowth into sheet-like structures, which can lead to the contraction of the hydrogel and eventual cell detachment.

Finally, a broad range of assays can be performed using this model. In addition to immunofluorescence and microscopy performed in live or fixed cultures, the 3D cultures may be enzymatically digested, and the cells can be retrieved and subjected to any type of biochemical assay. Here, we demonstrate the determination of ALP activity and DNA content quantification in cell lysates using colorimetric/fluorometric assays, but the system is compatible with many other techniques, including PCR, RNAseq, and proteomics. If the sensitivity of the desired assay is not very high, one can pool samples from more than one well to increase the amount of sample available for the assay. If the desired application requires faster gel dissolution, orbital shaking of the plate could be applied in combination with smaller volumes of the digestive solution to ensure vortex formation in the wells, assuming that all wells on the plate will be used in this manner (living cultures are sensitive to such harsh handling). In summary, we present here a protocol that, if used as described, guarantees the generation of an *in vitro* model that recapitulates the key aspects of osteogenic vascular niches but is also versatile enough to be modified for tailor-made applications.

Disclosures

Ectica Technologies AG is the manufacturer of the 3DProSeed hydrogel well plate and has commercial interests. Benjamin R. Simona and Martin Ehrbar are shareholders of Ectica Technologies AG.

Acknowledgments

The authors would like to thank Riccardo Urbanet for technical assistance with the liquid handling devices and Rodi Odabasi for support with the epifluorescence microscopy. This work was financed by the Swiss National Science Foundation (grant numbers 310030E_202429 and 205321_204318) and Ectica Technologies AG.

References

1. Mendez-Ferrer, S. et al. Mesenchymal and haematopoietic stem cells form a unique bone marrow niche. *Nature*. **466** (7308), 829-834 (2010).
2. Calvi, L. M., Link, D. C. Cellular complexity of the bone marrow hematopoietic stem cell niche. *Calcified Tissue International*. **94** (1), 112-124 (2014).
3. Behrmann, L., Wellbrock, J., Fiedler, W. Acute myeloid leukemia and the bone marrow niche-take a closer look. *Frontiers in Oncology*. **8**, 444 (2018).
4. Yip, R. K. H. et al. Mammary tumour cells remodel the bone marrow vascular microenvironment to support metastasis. *Nature Communications*. **12** (1), 6920 (2021).
5. Potente, M., Makinen, T. Vascular heterogeneity and specialization in development and disease. *Nature Reviews Molecular Cell Biology*. **18** (8), 477-494 (2017).
6. Augustin, H. G., Koh, G. Y. Organotypic vasculature: From descriptive heterogeneity to functional pathophysiology. *Science*. **357** (6353), eaal2379 (2017).
7. Kusumbe, A. P., Ramasamy, S. K., Adams, R. H. Coupling of angiogenesis and osteogenesis by a specific vessel subtype in bone. *Nature*. **507** (7492), 323-328 (2014).
8. Barillari, G. The anti-angiogenic effects of anti-human immunodeficiency virus drugs. *Frontiers in Oncology*. **10**, 806 (2020).
9. Owen, M., Friedenstein, A. J. Stromal stem-cells - Marrow-derived osteogenic precursors. *Ciba Foundation Symposia*. **136**, 42-60 (1988).
10. Sacchetti, B. et al. Self-renewing osteoprogenitors in bone marrow sinusoids can organize a hematopoietic microenvironment. *Cell*. **131** (2), 324-336 (2007).
11. Traore, M. A., George, S. C. Tissue engineering the vascular tree. *Tissue Engineering. Part B, Reviews*. **23** (6), 505-514 (2017).
12. Bessy, T., Itkin, T., Passaro, D. Bioengineering the bone marrow vascular niche. *Frontiers in Cell and Developmental Biology*. **9**, 645496 (2021).
13. Bray, L. J. et al. A three-dimensional ex vivo tri-culture model mimics cell-cell interactions between acute myeloid leukemia and the vascular niche. *Haematologica*. **102** (7), 1215-1226 (2017).
14. Montano, I. et al. Formation of human capillaries in vitro: The engineering of prevascularized matrices. *Tissue Engineering Part A*. **16** (1), 269-282 (2010).
15. Sun, Z. Y., Kemp, S. S., Lin, P. K., Aguera, K. N., Davis, G. E. Endothelial k-RasV12 expression induces capillary deficiency attributable to marked tube network expansion coupled to reduced pericytes and basement membranes. *Arteriosclerosis Thrombosis and Vascular Biology*. **42** (2), 205-222 (2022).
16. Kleinman, H. K. et al. Basement-membrane complexes with biological-activity. *Biochemistry*. **25** (2), 312-318 (1986).

17. Kubota, Y., Kleinman, H. K., Martin, G. R., Lawley, T. J. Role of laminin and basement-membrane in the morphological-differentiation of human-endothelial cells into capillary-like structures. *Journal of Cell Biology*. **107** (4), 1589-1598 (1988).
18. Davis, G. E. et al. Control of vascular tube morphogenesis and maturation in 3D extracellular matrices by endothelial cells and pericytes. *Methods in Molecular Biology*. **1066**, 17-28 (2013).
19. Jeon, J. S. et al. Human 3D vascularized organotypic microfluidic assays to study breast cancer cell extravasation. *Proceedings of the National Academy of Sciences of the United States of America*. **112** (1), 214-219 (2015).
20. Bersini, S. et al. A microfluidic 3D in vitro model for specificity of breast cancer metastasis to bone. *Biomaterials*. **35** (8), 2454-2461 (2014).
21. Wang, X. L. et al. Engineering anastomosis between living capillary networks and endothelial cell-lined microfluidic channels. *Lab on a Chip*. **16** (2), 282-290 (2016).
22. Phan, D. T. T. et al. A vascularized and perfused organ-on-a-chip platform for large-scale drug screening applications. *Lab Chip*. **17** (3), 511-520 (2017).
23. Lutolf, M. P., Hubbell, J. A. Synthetic biomaterials as instructive extracellular microenvironments for morphogenesis in tissue engineering. *Nature Biotechnology*. **23** (1), 47-55 (2005).
24. Kyburz, K. A., Anseth, K. S. Synthetic mimics of the extracellular matrix: How simple is complex enough? *Annals of Biomedical Engineering*. **43** (3), 489-500 (2015).
25. Ehrbar, M. et al. Enzymatic formation of modular cell-instructive fibrin analogs for tissue engineering. *Biomaterials*. **28** (26), 3856-3866 (2007).
26. Ehrbar, M. et al. Biomolecular hydrogels formed and degraded via site-specific enzymatic reactions. *Biomacromolecules*. **8** (10), 3000-3007 (2007).
27. Blache, U. et al. Dual role of mesenchymal stem cells allows for microvascularized bone tissue-like environments in PEG hydrogels. *Advanced Healthcare Materials*. **5** (4), 489-498 (2016).
28. Blache, U. et al. Notch-inducing hydrogels reveal a perivascular switch of mesenchymal stem cell fate. *Embo Reports*. **19** (8), e45964 (2018).
29. Simona, B. R. et al. Density gradients at hydrogel interfaces for enhanced cell penetration. *Biomaterials Science*. **3** (4), 586-591 (2015).
30. Zhang, N. et al. Soft hydrogels featuring in-depth surface density gradients for the simple establishment of 3d tissue models for screening applications. *SLAS Discovery*. **22** (5), 635-644 (2017).
31. Martin, I., Muraglia, A., Campanile, G., Cancedda, R., Quarto, R. Fibroblast growth factor-2 supports ex vivo expansion and maintenance of osteogenic precursors from human bone marrow. *Endocrinology*. **138** (10), 4456-4462 (1997).
32. Schindelin, J. et al. Fiji: An open-source platform for biological-image analysis. *Nature Methods*. **9** (7), 676-682 (2012).
33. Carpentier, G., Martinelli, M., Courty, J, Cascone, I. Angiogenesis Analyzer for ImageJ. *4th ImageJ User and Developer Conference*. 198-201. Mondorf-les-Bains, Luxembourg (2012).

34. Preibisch, S., Saalfeld, S., Tomancak, P. Globally optimal stitching of tiled 3D microscopic image acquisitions. *Bioinformatics*. **25** (11), 1463-1465 (2009).
35. Yamada, K. M., Cukierman, E. Modeling tissue morphogenesis and cancer in 3D. *Cell*. **130** (4), 601-610 (2007).
36. Loebel, C., Mauck, R. L., Burdick, J. A. Local nascent protein deposition and remodelling guide mesenchymal stromal cell mechanosensing and fate in three-dimensional hydrogels. *Nature Materials*. **18** (8), 883-891 (2019).
37. Curtis, M. B., Kelly, N., Hughes, C. C. W., George, S. C. Organotypic stromal cells impact endothelial cell transcriptome in 3D microvessel networks. *Scientific Reports*. **12** (1), 20434 (2022).
38. Wust, R., Terrie, L., Muntefering, T., Ruck, T., Thorrez, L. Efficient co-isolation of microvascular endothelial cells and satellite cell-derived myoblasts from human skeletal muscle. *Frontiers in Bioengineering and Biotechnology*. **10**, 964705 (2022).